Eur. Phys. J. C (2024) 84:60
https://doi.org/10.1140/epjc/s10052-024-12385-6

THE EUROPEAN PHYSICAL JOURNAL C

Regular Article - Theoretical Physics

Constant roll inflation and Finsler geometry: exploring anisotropic universe with scalar factor parametrization

S. K. Narasimhamurthy[a], **J. Praveen**[b]

Department of P.G Studies and Research in Mathematics, Kuvempu University, Shankaraghatta, Shivamogga, Karnataka 577 451, India

Received: 21 October 2023 / Accepted: 31 December 2023 / Published online: 20 January 2024

Abstract In this paper, we investigate the concept of cosmological constant-roll inflation within the framework of Finslerian space-time. We approach the theory of cosmic evolution using Finsler geometry, incorporating the parametrization of the anisotropic parameter by the scalar factor $a(t)$ by $\eta(t) = a(t)^{-n}$, where n is any real number. Our exploration mainly focuses on constant roll inflation, The analytical expression for Hubble parameter is found by using constant roll condition, and we derive crucial cosmological parameters such as scalar factor $a(t)$, scalar spectral index (n_s), and tensor-to-scalar ratio (r) for the inflationary universe. By using the analytical expressions for slow-roll parameters and the number of e-folds number we have found the values of n_s and r. Further, we identify the range of α values for which the theoretical values of spectral indices align with the observed Planck's data. This work significantly contributes to our understanding of inflationary dynamics within the context of Finsler geometry.

1 Introduction

In standard cosmology, inflation helps to address issues like the flatness and horizon problems, while quantum fluctuations of the inflaton field impact the universe large-scale structure and leave imprints on CMB radiation [1,2]. To tackle these cosmological challenges, it's essential to have a sufficient number of e-folds, typically set between 50 to 70 due to uncertainties in the underlying physics. The simplest form of inflation, known as slow-roll inflation, involves a scalar field slowly descending a nearly flat potential and is characterized by slow-roll parameters. An intriguing extension of slow-roll inflation is constant-roll inflation, which falls between slow roll and hill-top inflation in terms of its dynamics [3].

The standard cosmological model treats the universe as an adiabatically expanding radiation-dominated system. However, this model falls short in addressing key cosmological challenges such as the horizon, flatness, and monopole problems. To address and resolve these issues, Alan H. Guth proposed the concept of inflation in [3]. This inflationary model involves fluctuations in the scalar field during the universe's exponential expansion, leading to scalar density perturbations, as discussed in [4]. In [5], an alternative model for a large-scale, isotropic, and homogeneous universe was introduced based on the phase transition of the scalar Higgs field. This model also explores the amplitude of adiabatic perturbations and the duration of the de Sitter stage during universe expansion. Subsequent researchers, as referenced in [6–13], further developed and modified these concepts. The formalization of the slow-roll approximation, which defines slow-roll parameters in terms of the Hubble parameter and the scalar field's potential, was presented in [14]. Additionally, in [15], a broader approach to cosmological inflation, beyond the scope of the slow-roll approximation, was discussed.

Constant-roll inflation is an intriguing extension of slow-roll inflation. In slow-roll inflation models, both slow-roll parameters, which quantify the rate of change of the scalar field during inflation, are typically smaller than one throughout the inflationary period. On the other hand, constant-roll inflation is characterized by a specific condition $\ddot{\phi} = -\alpha H\dot{\phi}$, where α is a real constant. This condition sets it apart from the traditional slow-roll inflation dynamics. In the context of inflation, understanding the geometric properties of space-time is crucial. This includes considerations of curvature, which is a result of the gravitational field generated by the universe's fluid content. The concept of inflation and its dynamics are also studied within the framework of geometry. Riemannian geometry has been a successful tool in

[a] e-mail: sknmurthy@kuvempu.ac.in (corresponding author)
[b] e-mail: praveenjayarama1998@gmail.com

explaining various cosmological aspects of the universe. In this mathematical framework, the geometry of the universe is described using Riemannian manifolds, which provide insights into its structure and behavior. When, exploring inflation in the context of geometry, researchers have considered modified gravity theories like $f(R)$, $f(Q)$, $f(R,T)$, and others within the realm of Riemannian geometry. These theories propose modifications to Einstein's general theory of relativity, incorporating different functions of the Ricci scalar (R) or other geometric quantities. Such modifications are discussed to elucidate the phenomenon of constant-roll inflation and provide alternative explanations for the dynamics of the early universe. These discussions and investigations are documented in the scientific literature [16–21].

In the literature, specifically in [20], researchers delved into the concept of constant-roll inflation by utilizing the background Friedmann equations. They derived various scalar potentials and comprehensively explored the concepts of scalar and tensor perturbations both analytically and numerically. This detailed analysis helped in understanding the dynamics of constant-roll inflation. The findings and implications of constant-roll inflation, particularly the role of the inflationary constant parameter α, were further examined in [22]. The study involved a confrontation of these results with observational data to ascertain the viability and compatibility of the model with real-world cosmological observations. The inflationary constant parameter α was revealed to significantly influence the inflationary dynamics and was subjected to scrutiny against observational constraints. Moreover, the concept and implications of constant-roll inflation, particularly concerning the inflationary constant parameter α, have been thoroughly explored and discussed in subsequent research articles [23–27]. These studies elaborated on the constraints placed on α using essential cosmological parameters such as the scalar spectral index (n_s) and the tensor-to-scalar ratio (r). The interplay between α and these cosmological parameters helps refine our understanding of constant-roll inflation and its alignment with observational data.

Finsler geometry is a branch of differential geometry that doesn't impose quadratic restrictions on the metric tensor, as highlighted in references [28–31]. Researchers have explored the application of Finslerian geometry to the study of the universe, as discussed in [32,33]. This application has extended the Finslerian framework to incorporate the concept of inflation, aiming to provide an explanation for the observed anisotropy in the cosmic microwave background (CMB) spectra of the universe, as detailed in references [34–36]. Notably, the concept of constant-roll inflation within the context of Finslerian geometry was introduced for the first time in [37]. This pioneering work involved the use of Finsler–Rander's geometry to study the dynamics of constant-roll inflation, thereby contributing to a deeper understanding of the early universe inflationary processes within the framework of Finsler geometry.

In this paper, we delve into the concept of constant-roll inflation within the framework of Finsler geometry. More precisely, our focus is on exploring the idea of an inflationary universe within the context of Kropina spaces, as detailed in references [38–40]. Kropina spaces can be categorized as a type of Finsler spaces, and in our analysis, we employ the Barthel connection [41–44] to investigate these spaces. Our approach involves treating the space as an Osculating Riemannian space [45], which draws inspiration from the pioneering work conducted by researchers [46,47]. By applying these mathematical concepts and connections, we aim to gain a deeper understanding of the dynamics of constant-roll inflation in the unique backdrop of Finsler geometry, specifically within the framework of Kropina spaces.

The paper is structured as follows: In Sect. 2, we will present an overview of Finsler spaces, with a particular emphasis on Kropina spaces, and the Barthel connection. We will also introduce the fundamentals of cosmological inflation in this section. In Sect. 3, we will introduce our model and thoroughly explore the dynamics of cosmological inflation. Section 4 will be dedicated to a comprehensive discussion of our results in comparison to observational data. Finally, in Sect. 5, we will summarize and conclude our work presented in this paper.

2 Finsler geometry and cosmological inflation

Finsler geometry expands upon Riemannian geometry by considering a broader notion of distance between points in a space. In Riemannian geometry, distances are defined by the shortest curve connecting two points. Finsler geometry, however, allows for a distance function that incorporates both the direction and magnitude of displacement between points using the Finsler metric. Thus, Finsler space is a metric generalization of Riemann geometry

A Finsler space, explored in references [29–31,38,39], involves a manifold equipped with a Finsler metric function, denoted as F defined on the tangent bundle TM of the manifold. This function F satisfies the following properties

1. F is a smooth function on TM excluding the zero vectors and continuous on the null section of the projection $\pi : TM \to M$.
2. It exhibits positive homogeneity of order one with respect to the fiber coordinates.
3. The symmetric bilinear form

$$g_{ij}(x,y) = \frac{1}{2}\dot{\partial}_i\dot{\partial}_j F^2(x,y) \tag{1}$$

derived from F, is non-degenerate and has constant signature.

A manifold M of dimension n, equipped with the Finsler metric function F, constitutes a Finsler Space. In a Finsler space, the Cartan tensor C_{ijk} plays a crucial role. This tensor is derived from the Finsler metric and is analogous to the Christoffel symbol in Riemannian geometry. It characterizes geometric properties and can indicate whether the space reduces to Riemannian geometry ($C_{ijk} = 0$).

Furthermore, the Christoffel symbol in Finsler geometry, denoted as the $\gamma^i_{jk}(x, y)$, constructed from the fundamental tensor $g_{ij}(x, y)$, shares similarities with the Christoffel symbol in Riemannian geometry Γ^i_{jk}. Understanding Finsler geometry allows for a more general description of spaces, encompassing both Riemannian and non-Riemannian geometries. It provides a framework to study spaces with non-symmetric or anisotropic properties, offering a broader perspective on the geometry of manifolds. Within the realm of Finsler spaces, you can find various subtypes like Randers spaces and Kropina spaces among others.

In the field of Finsler geometry, various connections have been developed to enhance the understanding of these spaces. However, it's worth noting that computing geometric properties in Finsler spaces can be a complex task. To streamline these calculations and unlock the geometrical possibilities inherent in Finsler geometry, researchers frequently employ the osculating approach tailored for Finsler spaces [45]. This approach is particularly relevant in our investigation, where we focus on the application of Kropina spaces in gaining insights into the structure of the universe. Our specific interest lies in utilizing the Barthel connection within the framework of Kropina spaces [40]. This paper delves into the exploration of Finsler geometry, emphasizing its potential applications, especially in the context of Kropina spaces, as a means to advance our understanding of the universe's structural characteristics.

2.1 Kropina space and osculating Riemannian approach

The fundamental function $L = \frac{F^2}{2}$ of the Finsler metric which is homogeneous function of degree 1 in F. Here the $\alpha(x, y)$ Riemannian metric and $\beta(x, y)$ is the differential 1-form are defined by $\alpha(x, y) = \sqrt{a_{ij}(x) y^i y^j}$, $\beta = b_i(x) y^i$, is called the (α, β) metric. The space $R^n = (M^n, \alpha)$ is called associated Riemannian space and the covariant vector field b_i is the associated vector field. The Finsler fundamental function $L(x, y)$ defined by

$$L(x, y) = \frac{F^2}{2} = \frac{\alpha^2}{\beta} = \frac{a_{ij}(x) y^i y^j}{b_i(x) y^i}, \tag{2}$$

is called Kropina metric. By making the substitution (2) in (1), we derive the expression for the fundamental metric tensor $\hat{g}_{ij}(x, y)$ of the (α, β) space as follows

$$\hat{g}_{ij}(x, y) = \frac{L_\alpha}{\alpha} h_{ij} + \frac{L_{\alpha\alpha}}{\alpha^2} y_i y_j + \frac{L_{\alpha\beta}}{\alpha}\left(y_i b_j + y_j b_i\right) + L_{\beta\beta} b_i b_j, \tag{3}$$

with respect to above equation, $h_{ij} = \frac{\alpha \partial^2 \alpha(x,y)}{\partial y^i \partial y^j} = a_{ij} - \frac{y_i y_j}{\alpha^2}$ is angular metric tensor of the associate Riemannian space. L_{ij} denotes the partial derivative of L with respect to i, j.

When we introduce the Finsler metric $L(x, y)$ into a physical system alongside a non-zero vector field $Y(x)$, we observe the development of the Y-Riemannian metric $g(x)$ and as the result Barthel connection [41–44], which simplifies to the Levi-Civita connection. This sequence of transformations and connections allows us to investigate the physical system from the perspective of Riemannian geometry, providing a valuable approach for analysis and interpretation. Consequently, the curvature tensor associated with this affine connection, which features local coefficients denoted as $(\hat{\Gamma}^a_{bc})$, can be expressed as follows

$$\hat{R}^a_{bcd} = R^a_{bcd} = \frac{\partial \hat{\Gamma}^a_{bd}}{\partial x^c} - \frac{\partial \hat{\Gamma}^a_{bc}}{\partial x^d} + \hat{\Gamma}^e_{bd}\hat{\Gamma}^a_{ec} - \hat{\Gamma}^e_{bc}\hat{\Gamma}^a_{ed}. \tag{4}$$

And the Ricci curvature tensor is given by

$$\hat{R}_{bd} = \sum_a \left(\frac{\partial \hat{\Gamma}^a_{bd}}{\partial x^a} - \frac{\partial \hat{\Gamma}^a_{ba}}{\partial x^d} + \sum_E \hat{\Gamma}^e_{bd}\hat{\Gamma}^a_{ea} - \hat{\Gamma}^e_{ba}\hat{\Gamma}^a_{ed} \right). \tag{5}$$

With $a, b, c, d \in \{0, 1, 2, 3\}$. And the Ricci tensor and Ricci scalar are given by

$$\hat{R}^b_d = \hat{g}^{bc}\hat{R}_{cd} \quad , \quad \hat{R} = \hat{R}^a_{bad}. \tag{6}$$

The Barthel connection, characterized by its local coefficients $\left(b^a_{bc}\right)$, is a type of affine connection and is defined by

$$b^i_{kh} = (\gamma^i_{kh} - \gamma^r_{ks} Y^s C^i_{rh}).$$

As such, its curvature tensor can be determined using the aforementioned curvature formula (4), with the Christoffel symbols $\hat{\Gamma}^a_{bc}$.

2.2 Cosmological inflation and the osculating Finsler–Barthel–Kropina geometry approach

In this section, we explore the connection between cosmological inflation theory and the novel framework of the oscillating Finsler–Barthel–Kropina geometry. This innovative approach offers a unique perspective on the study of the early universe and its inflationary processes.

In the context of applying Barthel–Kropina geometry to cosmological inflation, we incorporate assumptions from

[46,47]. In this framework, the Riemannian metric $a_{ij}(x)$ within the Kropina metric $\alpha(x, y)$ is defined by the FLRW metric

$$a_{ij}(x) = dt^2 - a^2(t)(dx^2 + dy^2 + dz^2). \tag{7}$$

Here, $a(t)$ represents the cosmological scale factor. The FLRW metric describes a universe that is both homogeneous and isotropic, with cosmological time t progressing uniformly. The Barthel–Kropina metric components depend solely on cosmological time, aligning with the cosmological principle that attributes the universe large-scale attributes to time. This also implies that the 1-form β has components $(b^i) = (\eta(t), 0, 0, 0)$, with null spatial components.

Given the Kropina metric tensor described in Eq. (3), we choose a non-vanishing vector field $Y = A$, with $A^i = g^{ij} A_j$. Since the one-form β is defined across the entire manifold M and A is a globally defined non-vanishing vector field on M, it follows that the components of β are inherently non-zero. To address the complexities associated with the metric tensor, we adopt the Osculating Riemannian geometry approach. This leads us to the conclusion that $y_0 = y^0 = \eta(t)$, and $\alpha = \sqrt{a_{ij}(x)\, y^i\, y^j} = \sqrt{a_{ij}(x)\, A^i\, A^j}$, resulting in $\alpha^2 = a_{ij}(x)\, A^i A^j = A^2$. Additionally, we observe that $\beta = A_i y^i = A_i A^i = g_{ij}(x)\, A^i A^j = A^2 = \alpha^2$. Its evident that the metric is non-degenerate as $\eta(t)$ is non-zero.

This can be expressed as follows

i) $\beta = A_i y^i = \left(A^i\right) = (A_i) = (\eta(t), 0, 0, 0)$,
ii) $\left(\hat{g}_{ij}\right) = diag\left(1, -a^2(t), -a^2(t), -a^2(t)\right)$,
iii) $\alpha(x, y)\big|_{y=A(x)} = \eta(t)$,
iv) $\beta(x, y)\big|_{y=A(X)} = \eta(t)^2$.

This yields the following:

$$\hat{g}_{00} = \frac{2\alpha^2}{\beta^2} + \frac{3\alpha^4}{\beta^4}\eta^2 - \frac{8\alpha^2}{\beta^3} y_0 \eta + \frac{4}{\beta^2} y_0^2, \tag{8}$$

$$\hat{g}_{io} = -\frac{4\alpha^2}{\beta^3}\eta y_i + \frac{4}{\beta^2} y_i y_0, \tag{9}$$

$$\hat{g}_{ij} = -\frac{2a^2}{\beta^2}\left(\alpha^2 - 2a^2 y^i y^j\right)\delta^{ij}, \tag{10}$$

where $i, j \in \{1, 2, 3\}$.

Therefore, by introducing the A-osculating Riemannian manifold $(M, \hat{g}_{ij}(x, Y(x))$ on the manifold M, the metric components can be expressed as,

$$\left(\hat{g}_{ij}(x, y)\right) = diag\left(\frac{1}{\eta(t)^2}, -\frac{2a^2}{\eta(t)^2}, -\frac{2a^2}{\eta(t)^2}, -\frac{2a^2}{\eta(t)^2}\right). \tag{11}$$

The inverse metric tensor components can be represented as,

$$\left(\hat{g}^{ij}(x, y)\right) = diag\left(\eta(t)^2, -\frac{\eta(t)^2}{2a^2}, -\frac{\eta(t)^2}{2a^2}, -\frac{\eta(t)^2}{2a^2}\right). \tag{12}$$

2.3 Constant roll inflation

Inflationary models are characterized by a fundamental assumption known as the slow-roll assumption [14,22], where a scalar field gradually rolls down its potential. These models are described using dimensionless parameters referred to as slow-roll parameters. The smallness of these parameters during inflation ensures that the potential energy remains almost flat. These parameters are defined as follows:

$$\epsilon_1 = -\frac{\dot{H}}{H^2},$$
$$\epsilon_2 = \frac{\dot{\epsilon_1}}{H\epsilon_1}. \tag{13}$$

Constant-roll inflation represents a specific class of phenomenological models characterized by a constant rate of inflaton evolution, which can be expressed as

$$\ddot{\phi} = -\alpha H \dot{\phi}. \tag{14}$$

And we can also write second roll slow-roll parameter as

$$\epsilon_2 = 2\alpha + 2\epsilon_1. \tag{15}$$

and in general, the n^{th} slow roll parameters are given by $\epsilon_n = \frac{\dot{\epsilon_n}}{H\epsilon_n}$.

To induce inflation in the early universe, negative pressure is a prerequisite. This inflationary concept involves the presence of a spatially homogeneous scalar field $\phi = \phi(t)$, known as the inflaton. In the initial phases of the universe, this scalar field assumes a value where the potential $V(\phi)$ is both large and flat. As the scalar field evolves, it gradually moves down this potential, leading to a gradual reduction in the Hubble constant. This process triggers a period of inflation in the universe, characterized by an effective equation of state featuring negative energy and, consequently, negative pressure. This scalar field is introduced through a Lagrangian of a specific form [22,37]

$$\mathcal{L}_m = -\frac{1}{2} g^{\mu\nu}\partial_\mu\phi\partial_\nu\phi - V(\phi), \tag{16}$$

where $V(\phi)$ represents a certain potential function. Let us now examine the action governing inflation, which is propelled by a scalar field ϕ through minimal coupling. This action is given by

$$\mathcal{L} = \int dx^4\sqrt{-\hat{g}}\left(\frac{M_{pl}^2}{2}\hat{R} + \mathcal{L}_m\right). \tag{17}$$

In this context, $\sqrt{-\hat{g}}$ represents the determinant of the osculating Barthel–Kropina–Finsler metric, and $\hat{R}$ is the Ricci scalar associated with the Osculating Finsler–Barthel–Kropina metric. When we vary the action with respect to the metric tensor, this procedure yields the Einstein field equation [1,2], which can be expressed as follows

$$\hat{R}_{ij} - \frac{1}{2}\hat{g}_{ij}\hat{R} = k\hat{T}_{ij}. \tag{18}$$

Where, $\hat{R}_{ij}$ is the components of Ricci tensor, $\hat{R}$ is the component Ricci scalar of the metric tensor defined by the equation (16) and $k = \frac{1}{M_{pl}^2}$.

The computation of the various geometric quantities in the context of cosmological spacetime which is given in the appendix. With the previously mentioned osculating Kropina metric, the generalized Friedmann equations can be expressed as follows

$$3\dot{\eta}^2 + 3\eta^2 H^2 - 6\eta\dot{\eta}H = \frac{\rho}{M_{pl}^2}, \tag{19}$$

$$-3\dot{\eta}^2 - 3\eta^2 H^2 + 4\eta\dot{\eta}H - 2\eta^2\dot{H} + 2\eta\ddot{\eta} = \frac{p}{M_{pl}^2}. \tag{20}$$

The equations presented differ from those in [46] due to our selection of a specific 1-form. However, these equations can be regained by adopting a particular choice of the 1-form inherent in the Finslerian Kropina metric.

Finsler geometry provides an extra term η and its derivatives compared to that of Riemannian case which in turn explain the advantage of Finsler geometry over Riemannian case. Inflationary models heavily rely on the properties of spacetime geometry. Introducing a Kropina metric with an additional 1-form term $\eta(t)$ alters the geometry of spacetime. Depending on the specific form of $\eta(t)$, it affects the expansion rate, curvature, and evolution of the early universe during inflation. The modification introduced by the Kropina metric influence the dynamics of inflation. It's impact on the scalar field responsible for inflation, altering its potential or its interactions with other fields. This modification could lead to variations in the duration and properties of inflation, affecting the resulting cosmological predictions. Inflationary models make predictions about observable signatures such as primordial gravitational waves, density fluctuations, and non-Gaussianities in the cosmic microwave background. Modifications introduced by the Kropina metric result in distinct signatures compared to standard inflationary models based on Riemannian metrics, potentially offering observational tests to distinguish between different cosmological scenarios.

And the Klein–Gordon equation of motion is given by

$$\ddot{\phi} + \dot{\phi}\left(3H - 4\frac{\dot{\eta}}{\eta}\right) + V_\phi = 0. \tag{21}$$

And $\hat{T}_{ij}$ is the components of energy momentum tensor, defined as

$$\hat{T}_{ij} = \frac{-2}{\sqrt{-\hat{g}}}\frac{\delta\left(\sqrt{-\hat{g}}\mathcal{L}_m\right)}{\delta\hat{g}^{ij}} = \hat{g}_{ij}\mathcal{L}_m - \frac{2\delta\mathcal{L}_m}{\delta\hat{g}^{ij}}, \tag{22}$$

which is equivalent to

$$\hat{T}^i_j = \hat{g}^{ik}\phi_{,k}\phi_{,j} - \left(\frac{1}{2}\hat{g}^{lm}\phi_{,l}\phi_{,m} - V(\phi)\right)\delta^i_j. \tag{23}$$

The energy density of the cosmological matter and thermodynamical pressure are given respectively as,

$$\rho = \hat{T}^0_0 = \frac{1}{2}\hat{g}^{00}\dot{\phi}^2 + V, \tag{24}$$

$$p = \hat{T}^i_i = \frac{1}{2}\hat{g}^{00}\dot{\phi}^2 - V. \tag{25}$$

Substituting the above expression for energy density and pressure the Friedmann equations becomes,

$$3\dot{\eta}^2 + 3\eta^2 H^2 - 6\eta\dot{\eta}H = \frac{1}{M_{pl}^2}\left(\frac{1}{2}\eta^2\dot{\phi}^2 + V\right), \tag{26}$$

$$-3\dot{\eta}^2 - 3\eta^2 H^2 + 4\eta\dot{\eta}H - 2\eta^2\dot{H} + 2\eta\ddot{\eta} = \frac{1}{M_{pl}^2}\left(\frac{1}{2}\eta^2\dot{\phi}^2 - V\right). \tag{27}$$

Adding above two equations we get

$$\dot{\phi}^2 + 2M_{pl}^2\dot{H} + 2M_{pl}^2\left(H\frac{\dot{\eta}}{\eta} - \frac{\ddot{\eta}}{\eta}\right) = 0. \tag{28}$$

The distinctiveness of the Friedmann equations and the equation of motion, in contrast to the Riemannian scenario, is quite apparent from Eqs. (26)–(28). And, as $\eta \to 1$ the equation these equations reduce to Riemannian case, and the dynamics of inflation is same as Riemannian case. Thus $\eta(t)$ deviates the homogenous, isotropic universe in Riemannian case to large scale homogeneous, isotropic structure which in small case is anisotropic. Thus, these variations can be attributed to the existence of a Finslerian metric that depends on direction and the introduction of the anisotropic term $\eta(t)$. The introduction of $\eta(t)$ within the Kropina metric can indeed be interpreted as introducing an anisotropic element into the geometry of spacetime. Anisotropy refers to variations in different directions within the universe. When $\eta(t)$ is included in the Kropina metric, it introduces a direction-dependent component that varies with time t. This time-dependent term $\eta(t)$ modifies the structure of spacetime in a manner that can be considered anisotropic, especially if it affects different spatial directions differently. The anisotropy might manifest as a directional preference or variation in the geometry, impacting the expansion rate or curvature along specific axes or directions in space.

Anisotropies can have significant implications, affecting the predictions of observational phenomena such as the

cosmic microwave background radiation, large-scale structure formation, and the overall evolution of the universe. Therefore, interpreting $\eta(t)$ within the Kropina metric as an anisotropic term allows for the consideration of scenarios where the universe's geometry exhibits direction-dependent characteristics, potentially deviating from the isotropic properties usually assumed in standard cosmological models based on Riemannian metrics.

Obtaining an analytical solution for $\eta(t)$ directly from the deductions of the Einstein Field equations or other equations governing cosmological dynamics in a Finslerian background is often a challenging task. To facilitate the analysis of inflationary dynamics in our study, we have proposed a model in which $\eta(t)$ takes the form $\eta(t) = a(t)^{-n}$ [46]. This simplification allows us to streamline the governing equations and gain insights into the inflationary behavior.

3 The model with $\eta(t) = a(t)^{-n}$

In the context of the specified model, the Eq. (28) can be expressed as

$$\dot{\phi}^2 + 2(1+n) M_{pl}^2 H' \dot{\phi} - 2M_{pl}^2 n (n+1) H^2 = 0, \tag{29}$$

where we treat H as a function of ϕ. Where prime denotes the derivative with respect to ϕ. Clearly, the above equation is qudratic in $\dot{\phi}$ and its roots are given by

$$\dot{\phi} = -(1+n) M_{pl}^2 H' \pm \sqrt{(n+1)^2 M_{pl}^4 H'^2 + 2n(n+1) M_{pl}^2 H^2}. \tag{30}$$

Again, differentiating the above expression with respect to cosmic time and using the constant roll condition, $\ddot{\phi} = -\alpha H \dot{\phi}$, we get

$$-\alpha H = -(1+n) M_{pl}^2 H'' \pm \frac{H' \left[(n+1)^2 M_{pl}^2 H'' + 2n(n+1) H\right]}{\sqrt{(n+1)^2 M_{pl}^2 H'' + 2n(n+1) H^2}}. \tag{31}$$

Using the above two solutions we obtain two differential equations

$$\alpha H = (n+1) M_{pl}^2 H'', \tag{32}$$

$$H'' = -\frac{2nH}{(n+1) M_{pl}^2}. \tag{33}$$

By considering the above two equations one can find that

$$n = -\frac{\alpha}{2}. \tag{34}$$

Therefore, the differential equation becomes

$$H'' = \frac{2\alpha H}{(2-\alpha) M_{pl}^2}, \tag{35}$$

the general solution of this equation is given by

$$\text{Case 1: } H(\phi) = M e^{\pm\sqrt{\frac{2\alpha}{2-\alpha}} \frac{\phi}{M_{pl}}} \tag{36}$$

$$\text{Case 2: } H(\phi) = M \cosh\left(\sqrt{\frac{2\alpha}{2-\alpha}} \frac{\phi}{M_{pl}}\right) \quad \text{if } \alpha \in (0,2), \tag{37}$$

$$H(\phi) = M \cos\left(\sqrt{\frac{2|\alpha|}{|2-\alpha|}} \frac{\phi}{M_{pl}}\right) \quad \text{if } \alpha \in (-\infty, 0) \cup (2, \infty), \tag{38}$$

$$\text{Case 3: } H(\phi) = M \sinh\left(\sqrt{\frac{2\alpha}{2-\alpha}} \frac{\phi}{M_{pl}}\right) \quad \text{if } \alpha \in (0,2), \tag{39}$$

$$H(\phi) = M \sin\left(\sqrt{\frac{2|\alpha|}{|2-\alpha|}} \frac{\phi}{M_{pl}}\right) \quad \text{if } \alpha \in (-\infty, 0) \cup (2, \infty). \tag{40}$$

Inflation is characterized by the gradual descent of the inflaton field along its potential energy curve, a condition expressed as $\dot{\phi}(t) \ll 1$ [1,2]. This condition implies that $\dot{\phi}(t)^2$ is extremely small. Based on this observation, we can simplify our analysis by approximating $\dot{\phi}^2(t) \approx 0$ during inflation.

Then the above equation yields that

$$2(n+1) M_{pl}^2 \dot{H} \dot{\phi} - 2M_{pl}^2 n (n+1) H^2 = 0. \tag{41}$$

Which gives us the expression for $\dot{\phi}$ as

$$\dot{\phi} = -\frac{\alpha}{2} \frac{H(\phi)^2}{H'(\phi)}. \tag{42}$$

By substituting the expressions for $H(\phi)$ from Eqs. (37)–(41) we obtain expressions for $\phi(t)$.

More importantly in this paper we discuss the Hubble function of the form (39)

$$H(\phi) = M \cos\left(\sqrt{\frac{2|\alpha|}{|2-\alpha|}} \frac{\phi}{M_{pl}}\right) \quad \text{if } \alpha \in (-\infty, 0) \cup (2, \infty).$$

Then the cosmological parameters are given by

$$\phi(t) = \sqrt{\frac{|2-\alpha|}{|2\alpha|}} \operatorname{arcsec}\left(\frac{|\alpha| Mt}{2}\right), \tag{43}$$

$$H(t) = \frac{2\left(M^2\alpha^2 t^2 - 2\right)}{\alpha t \left(M^2\alpha^2 t^2 - 4\right)}. \tag{44}$$

Graphs representing the dynamics of $H(t)$ and $a(t)$ have been plotted for a specific α value of -0.005, as illustrated in the Figs. 1 and 2.

The conventional method for analyzing inflation is through the use of the slow-roll approximation, where we define the slow-roll parameters as described in Eq. (13). During this approximation, it is assumed that these parameters are exceedingly small, satisfying the condition $|\epsilon_n| \ll 1$. Once the slow-roll parameters approach unity, the inflationary expansion comes to an end.

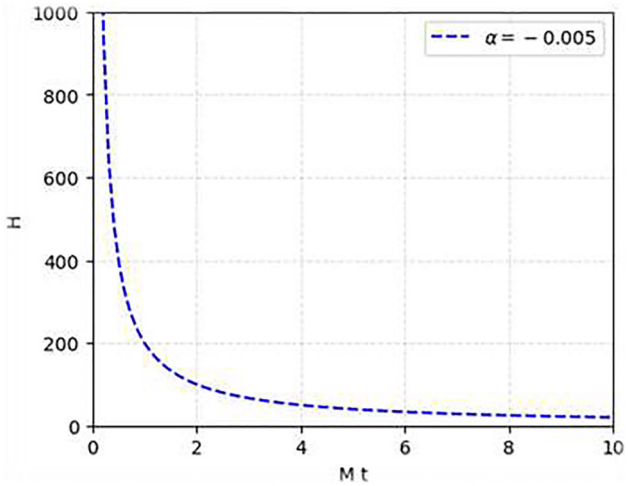

Fig. 1 The variation of hubble parameter (H) with the cosmic time (t)

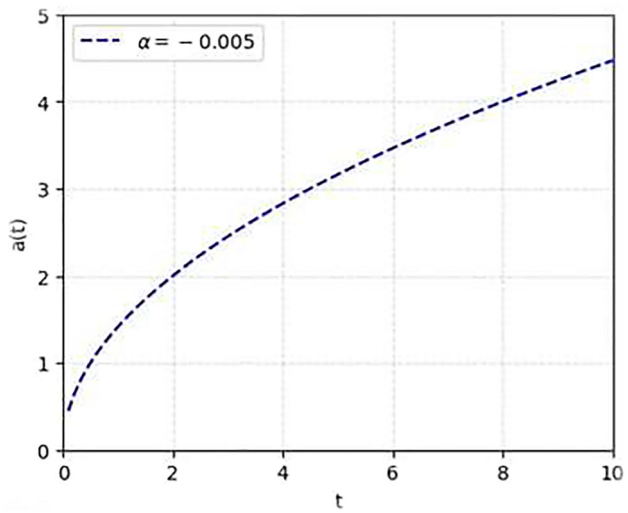

Fig. 2 The variation of scalar factor ($a(t)$) with the cosmic time (t)

These parameters, in turn, provide us with two key inflationary parameters one is the scalar spectral index(n_s) and another one is the tensor-to-scalar ratio (r) and they are given by [28]

$$n_s = 1 - 2\epsilon_1 - \epsilon_2, \tag{45}$$

$$r = 16\epsilon_1. \tag{46}$$

In our model, we have calculated the first two slow-roll parameters using the expression for $H(t)$ as described earlier. These parameters have been depicted graphically in the figure. Notably, it can be observed that for $\alpha = -0.005$, the inflationary slow-roll parameters approach zero, indicating the presence of inflationary phenomena.

Assessing slow-roll parameters precisely at the horizon crossing ($k = a\,H$), where the wave vector aligns with the product of the scale factor and the Hubble parameter is crit-

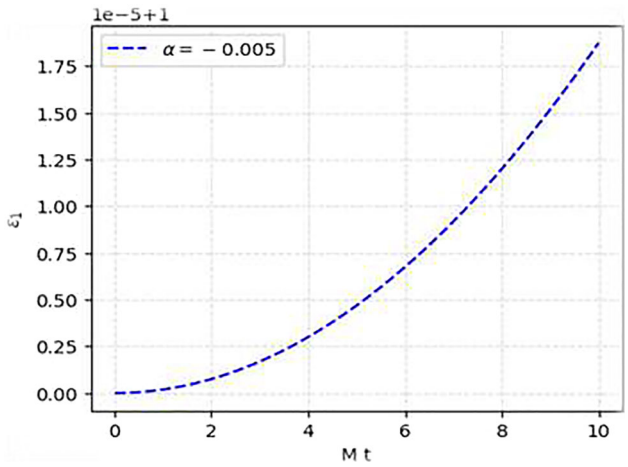

Fig. 3 The variation of first slow-roll parameter (ϵ_1) with the cosmic time (t)

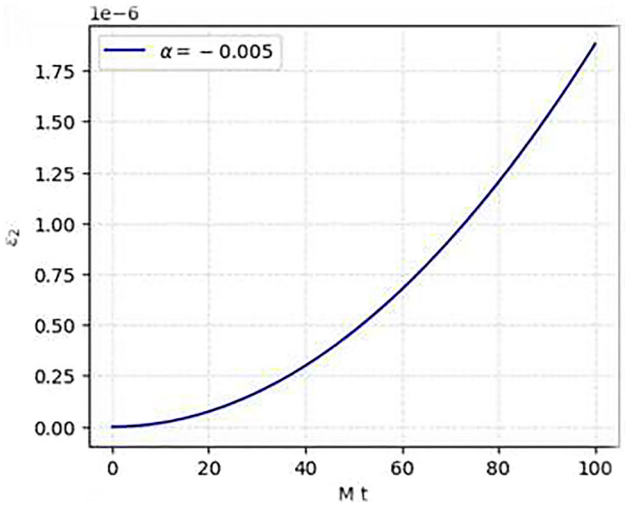

Fig. 4 The variation of second slow-roll parameter (ϵ_2) with the cosmic time (t)

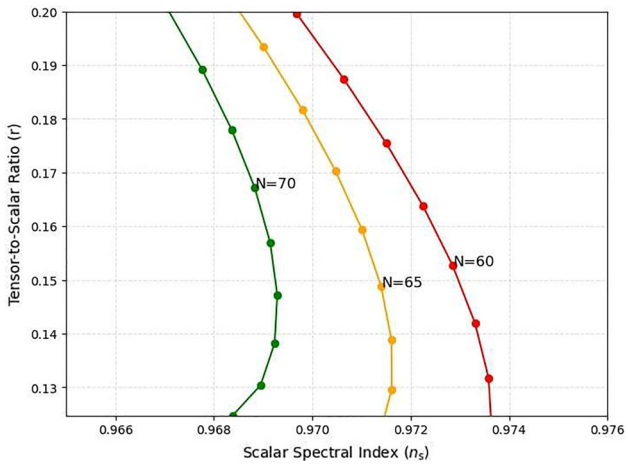

Fig. 5 Scalar spectral index (n_s) vs tensor-to-scalar ratio (r) for the data given in table 1

Table 1 Values of scalar-spectral index (n_s) and scalar-to-tensor ratio (r) for $\alpha \in [-0.001, -0.0001]$

$N = 60$			$N = 65$		$N = 70$	
α	n_s	r	n_s	r	n_s	r
− 0.0001	0.96738265	0.12654348	0.96988911	0.11673104	0.97203938	0.1083199
− 0.0002	0.96756555	0.12509758	0.97006531	0.11540087	0.97220974	0.10709287
− 0.0003	0.96770881	0.12434338	0.97020357	0.11473497	0.97234353	0.10650564
− 0.0004	0.96783175	0.12394529	0.97032229	0.11441097	0.97245847	0.10624763
− 0.0005	0.96794164	0.12377375	0.97042841	0.11430444	0.97256118	0.10619901
− 0.0006	0.96804208	0.12376253	0.97052531	0.11435179	0.97265487	0.10629853
− 0.0007	0.96813505	0.12387241	0.97061487	0.11451537	0.9727413	0.10650994
− 0.0008	0.96822188	0.12407788	0.97069834	0.11477072	0.97282167	0.10680972
− 0.0009	0.96830337	0.12436132	0.9707765	0.11510091	0.9728967	0.10718156
− 0.001	0.96838014	0.12470992	0.97084988	0.11549366	0.97296691	0.10761367

Table 2 Values of scalar-spectral index (n_s) and scalar-to-tensor ratio (r) for $\alpha \in [-0.01, -0.001]$

$N = 60$			$N = 65$		$N = 70$	
α	n_s	r	n_s	r	n_s	r
− 0.0001	0.96838014	0.12470992	0.97084988	0.11549366	0.97296691	0.10761367
− 0.0002	0.96894883	0.13038452	0.9713796	0.12152484	0.97345927	0.11396325
− 0.0003	0.96923437	0.13820373	0.97161459	0.12962379	0.97364545	0.12231352
− 0.0004	0.96928884	0.14716662	0.97160894	0.13883331	0.97358215	0.13174638
− 0.0005	0.96914484	0.15689672	0.97139825	0.14879399	0.97330809	0.14191757
− 0.0006	0.96882844	0.16720558	0.97101104	0.15932593	0.97285418	0.15265472
− 0.0007	0.9683613	0.17798324	0.97047076	0.170324	0.97224546	0.16385684
− 0.0008	0.96776157	0.18915875	0.96979671	0.18172009	0.9715023	0.17545814
− 0.0009	0.96704439	0.20068283	0.96900487	0.19346652	0.97064133	0.18741218
− 0.001	0.96622252	0.21251916	0.96810848	0.20552785	0.96967622	0.19968402

ical in inflationary cosmology. This moment marks the shift of quantum fluctuations in the scalar field from smaller to cosmologically significant scales. These fluctuations freeze as they leave the horizon during inflation, imprinting characteristics on the evolving universe. Studying slow-roll parameters here is crucial for understanding how primordial density perturbations form, evolve, and shape large-scale cosmic structures. This assessment facilitates the determination of power spectra, aiding in the comparison between theoretical predictions and empirical observations, thereby validating or constraining various inflationary models. Consequently, the evaluation of slow-roll parameters at the horizon crossing point is foundational in corroborating the consistency and viability of inflationary theories while unraveling the mysteries of the universe's early evolution and structure formation [1]. Thus, we assume that inflation initiates at the moment when field fluctuations become crucial during the horizon crossing. Therefore, the number of $e-$foldings, denoted as N and determining the extent of inflation, can be expressed as [25],

$$N = \int_{t_*}^{t_e} H\,(t)\,dt. \tag{47}$$

In the above equation, t_* and t_e denote the horizon crossing time and the end of inflation time, respectively. In terms of the scalar field, the equation can be expressed as

$$N = \int_{\phi_*}^{\phi_e} \frac{H}{\dot{\phi}} d\phi. \tag{48}$$

In order to determine the value of N at the conclusion of inflation, we initiate the calculation at the moment of horizon crossing ϕ_* by evaluating the slow-roll parameters. These calculated values are subsequently employed in the aforementioned equation.

4 Results and discussion

In this section, we discuss some important outcomes of our model. According to the latest data from Planck [48], the

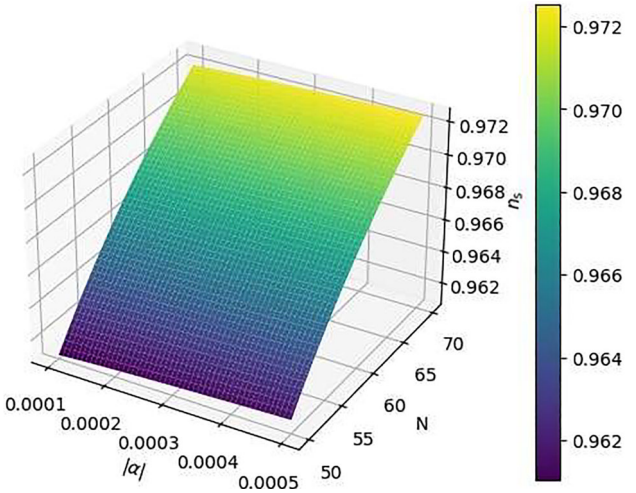

Fig. 6 The behavior of the scalar-spectral index (n_s) parameter is represented. We have choosen the range of $|\alpha|$ to be in $[0.0001, 0.0005]$ and N to be $[50, 70]$

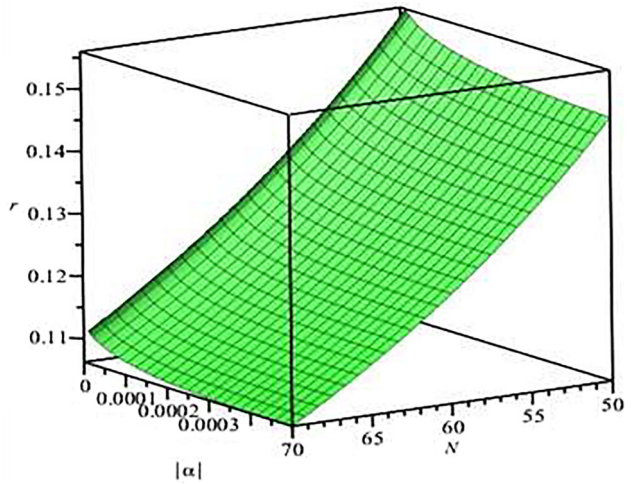

Fig. 7 The behavior of the scalar-to-tensor ratio (r) parameter is represented. We have choosen the range of $|\alpha|$ to be in $[0.0001, 0.0005]$ and N to be $[50, 70]$

range of the scalar spectral index parameter and the tensor-to-scalar ratio is as follows

$$n_s = 0.968 \pm 0.006 \text{ and } r < 0.12. \tag{49}$$

Inflation theory informs us that inflation concludes when the first slow-roll parameter $\epsilon_1 = 1$ i.e., $\epsilon_1(\phi_{end}) = 1$. By utilizing the inflationary parameters and the definition of ϵ_1 as given in Eq. (13), we can calculate the value of ϕ_{end}. Additionally, we determine the value of the inflaton at the horizon crossing by employing Eq. (48), which provides us with the value of ϕ_* in terms of the number of e-folding numbers (N). To compute the values of n_s and r, we evaluate ϵ_1 and ϵ_2 at $\phi = \phi_*$. Subsequently, using these expressions, we calculate the values of n_s and r for various N values.

Figure 1 illustrates the behavior of the Hubble parameter (H) for $\alpha = -0.005$. The plot clearly shows that the Hubble parameter approaches zero as time evolves, which is a characteristic signature of the inflationary phase. Furthermore, the scalar factor follows an evolution pattern akin to de-Sitter spacetime. In Fig. 2, we can observe that the universe is experiencing an accelerating expansion. Further we examine the slow-roll parameters, as shown in Figs. 3 and 4 for $\alpha = -0.005$. These plots reaffirm the essence of slow-roll inflation, with the slow-roll parameters remaining negligible throughout the inflationary period.

Figure 5 presents the relationship between the scalar spectra index(n_s) against scalar-to-tensor ratio (r) for different e-folding numbers ($N = 60, 65, 70$) and for α values spanning from -0.01 to -0.001. Strikingly, the results exhibit a remarkable agreement with the values of n_s and r specified in Equation (49). Furthermore, we assess the values of n_s and r at the horizon crossing. Across a range of values for α within the interval $[-0.01, -0.001]$, we have computed and presented the spectral index (n_s) and tensor-to-scalar ratio (r) in the accompanying graphs. Remarkably, our proposed model exhibits a substantial agreement with the established values of n_s and r given in equation (50). This observation underscores the validity of our model within the context of the scalar factor parametrization of the anisotropic parameter, particularly within the osculating Barthel-Kropina-Finslerian background, for this α the n values fall within the range of $n \in [-0.005, -0.0005]$.

Tables 1 and 2 offer a quantitative summary of our results. Table 1 lists the precise values of n_s and r for $\alpha \in [-0.001, -0.0001]$ across various N values. Table 2 extends this analysis to encompass $\alpha \in [-0.001, -0.01]$. Notably, the values in Table 1 exhibit a closer alignment with observed data, reaffirming the robustness of our model. For more visual representation, we have included the graphical evidence in Figs. 6 and 7 for the range of α values within $[-0.001, -0.0001]$

5 Conclusion

In this paper, we have extensively explored the concept of constant-roll inflation within the framework of Finsler geometry, with a particular focus on the Kropina space, one of the significant Finsler spaces. This investigation involved embedding the crucial Finslerian connection, the Barthel connection, within the context of Osculating Riemannian spaces. We derived important cosmological dynamics through this approach. By imposing the condition for constant-roll inflation and parametrizing the anisotropic parameter using the scalar factor, we obtained cosmological parameters that have not been previously explored in the study of the cosmological structure of the Universe. We fur-

ther examined the impact of these parameters on the slow-roll parameters and utilized standard expressions for the scalar spectral index and the tensor-to-scalar ratio. Additionally, we incorporated the expression for the number of e-folding in inflation to calculate cosmological spectral indexes for various values of N. The analysis revealed the range of α values for which our model aligns with the standard values of n_s and r. Remarkably, our results demonstrated a high degree of consistency with the standard Planck's data, highlighting the potential of Finslerian Kropina spaces as a framework for describing the evolution of the Universe.

Inflation, a period of rapid cosmic expansion preceding Big Bang nucleosynthesis, is believed to be driven by an inflaton scalar field. While there's been speculation about the inflaton being a form of dark energy, practical evidence shows the inflaton decays during inflation, making this unlikely. However, the dynamics of dark energy can be explored by using the equations describing inflationary scenarios. Numerous studies in the literature have investigated the relationship between dark energy and inflation [49–51]. Future research will delve into the connection between dark energy and inflation within the framework of Finslerian geometry, as previously explored by researchers [46,52,53]. Further this study opens up new avenues for exploring the Universe's dynamics within the context of Finsler geometry, offering a fresh perspective on cosmology.

Acknowledgements Praveen J and S K Narasimhamurthy acknowledges the Department of Science and Technology (DST) in New Delhi, India, for providing research facility support through DST-FIST-2019. The authors express their sincere gratitude to the anonymous reviewer for their valuable suggestions, which significantly improved the quality and presentation of the research.

Author contributions JP: conceptualization, formal analysis, methodology, writing-original draft. SKN: visualization, supervision, project administration, investigation.

Funding No funding was received for this research.

Data Availability Statement This manuscript has no associated data or the data will not be deposited. [Authors' comment: All the data included in this manuscript are available upon request by contacting with the corresponding author.]

Declarations

Conflict of interest The authors confirm that there are no financial interests or personal affiliations that could have influenced the research presented in this paper.

Funded by SCOAP^3.

Appendix

Computation geometrical properties of Osculating Finsler–Barthel–Kropina metric

The fundamental metric tensor of the Kropina metric is given by

$$\hat{g}_{ij}(x,y) = \frac{L_\alpha}{\alpha}h_{ij} + \frac{L_{\alpha\alpha}}{\alpha^2}y_i y_j + \frac{L_{\alpha\beta}}{\alpha}\left(y_i b_j + y_j b_i\right) + L_{\beta\beta}b_i b_j. \tag{A1}$$

with respect to above equation, $h_{ij}=\frac{\alpha\partial^2\alpha(x,y)}{\partial y^i\partial y^j}=a_{ij}-\frac{y_i y_j}{\alpha^2}$ is angular metric tensor of the associate Riemannian space. L_{ij} denotes the partial derivative of L with respect to i, j.

The Riemannian metric tensor α is given by the metric tensor

$$\left(a_{ij}(x)\right) = \begin{pmatrix} 1 & 0 & 0 & 0 \\ 0 & -a^2(t) & 0 & 0 \\ 0 & 0 & -a^2(t) & 0 \\ 0 & 0 & 0 & -a^2(t) \end{pmatrix}. \tag{A2}$$

And the one form of the Kropina metric as discussed is given by

$$\beta = (\eta(t),\ 0,\ 0,\ 0).$$

Utilizing the osculating Riemannian approach outlined in Sect. 2, the previously mentioned metric tensor simplifies into the osculating Barthel–Kropina metric given by

$$\hat{g}_{ij}(x) = \begin{cases} \eta^2 & if\ i=j=0 \\ -\frac{\eta^2}{2a^2}\ \delta_{ij} & if\ i=j=1,2,3 \end{cases}, \tag{A3}$$

$$\left(\hat{g}^{ij}(x,y)\right) = diag\left(\eta^2, -\frac{\eta^2}{2a^2}, -\frac{\eta^2}{2a^2}, -\frac{\eta^2}{2a^2}\right). \tag{A4}$$

Calculation of Finslerian geometrical quantities of Barthel–Kropina spaces

Christoffel symbol

The Finslerian Christoffel symbol is calculated with the help of Riemannian Christoffel symbol Γ^i_{jk} as we discussed above

and is given by,

$$\gamma_{ijk}\,(x,\,y)=\frac{1}{2}\left[\frac{\partial g_{jk}}{\partial x^i}+\frac{\partial g_{ki}}{\partial x^j}-\frac{\partial g_{ij}}{\partial x^k}\right]. \tag{A5}$$

Now g_{ij} is replaced by the metric tensor $\hat{g}_{ij}$. From the theory of Barthel connection, the Christoffel symbol of the osculating Barthel–Kropina metric is given by

$$\Gamma^i_{jk}=\gamma^i_{jk}=\frac{1}{2}g^{li}\left(\frac{\partial \hat{g}_{lk}}{\partial x^j}+\frac{\partial \hat{g}_{lj}}{\partial x^k}-\frac{\partial \hat{g}_{jk}}{\partial x^l}\right) \tag{A6}$$

And after further simplification we have

$$\begin{aligned}\hat{\Gamma}^i_{jk} &= \Gamma^i_{jk}\\ &= \begin{cases} -\frac{\dot{\eta}}{\eta} & if\ i=j=k=0.\\ -\frac{2a(\dot{\eta}a-\dot{a}\eta)}{\eta}\delta_{jk} & if\ i=0,\ j=k=1,\ 2,\ 3.\\ \frac{\dot{a}\eta-\dot{\eta}a}{\eta a}\,\delta_{jk} & if\ i=1,2,3,\ j=k=1,\ 2,\ 3.\end{cases}\end{aligned} \tag{A7}$$

Ricci tensor

The Ricci tensor is calculated using the Christoffel symbols and is given by,

$$\begin{aligned}\hat{R}_{bd} &= R_{bd}=\sum_a\left(\frac{\partial\Gamma^a_{bd}}{\partial x^a}-\frac{\partial\Gamma^a_{ba}}{\partial x^d}\right.\\ &\left.+\sum_E\Gamma^e_{bd}\Gamma^a_{ea}-\Gamma^e_{ba}\Gamma^a_{ed}\right).\end{aligned} \tag{A8}$$

This leads to

$$\hat{R}_{00}=R_{00}=\frac{\left(-3\ddot{a}\eta^2+3\ddot{\eta}\eta a+3\dot{\eta}\dot{a}\eta-3\dot{\eta}^2a\right)}{a\eta^2}, \tag{A9}$$

$$\begin{aligned}\hat{R}_{ij} &= R_{ij}\\ &= \frac{2\ddot{a}a\eta^2-2\ddot{\eta}\eta a^2+4\dot{a}\eta^2-10\dot{a}\dot{\eta}\eta a+6\eta^2a^2}{\eta^2}\delta_{ij}.\end{aligned} \tag{A10}$$

The generalized Friedmann equations

The Einstein Field equations are given by

$$\hat{G}_{ij}=\hat{R}_{ij}-\frac{1}{2}g_{ij}R, \tag{A11}$$

Eq. (A10) gives

$$\hat{G}_{00}=\frac{3\,(\dot{\eta}a-\dot{a}\eta)^2}{\eta^2a^2}, \tag{A12}$$

$$\hat{G}_{ij}=\frac{-4\eta^2a\ddot{a}-2\eta^2\dot{a}^2+4\eta a^2\ddot{\eta}+8\eta a\dot{a}\dot{\eta}-6a^2\dot{\eta}^2}{\eta^2}\delta_{ij}. \tag{A13}$$

The expression for generalized Friedmann equations is given by

$$\hat{G}_{00}=\frac{1}{M^2_{pl}}\,\hat{g}_{oo}\rho,\quad \hat{G}_{ii}=\frac{1}{M^2_{pl}}\,\hat{g}_{ii}\rho. \tag{A14}$$

Using Eqs. (A4)

$$3\dot{\eta}^2+3\eta^2H^2-6\eta\dot{\eta}H=\frac{\rho}{M^2_{pl}}, \tag{A15}$$

$$-3\dot{\eta}^2-3\eta^2H^2+4\eta\dot{\eta}H-2\eta^2\dot{H}+2\eta\ddot{\eta}=\frac{p}{M^2_{pl}}. \tag{A16}$$

References

1. A.R. Liddle, D.H. Lyth, *Cosmological Inflation and Large-scale Structure* (Cambridge University Press, Cambridge, 2000)
2. S. Dodelson, F. Schmidt, *Modern Cosmology* (Academic press, Cambridge, 2020)
3. A.H. Guth, Inflationary Universe: a possible solution to the horizon and flatness problems. Quantum Cosmol **3**, 139 (1987)
4. A.H. Guth, S.Y. Pi, Fluctuations in the new inflationary universe. Phys. Rev. Lett. **49**(15), 1110 (1982)
5. A.A. Starobinsky, Relict gravitation radiation spectrum and initial state of the universe. JETP Lett. **30**(682–685), 131–132 (1979)
6. A.A. Starobinsky, A new type of isotropic cosmological models without singularity. Phys. Lett. B **91**(1), 99–102 (1980)
7. A.A. Starobinsky, Dynamics of phase transition in the new inflationary universe scenario and generation of perturbations. Phys. Lett. B **117**(3–4), 175–178 (1982)
8. A.D. Linde, A new inflationary universe scenario: a possible solution of the horizon, flatness, homogeneity, isotropy and primordial monopole problems. Phys. Lett. B **108**(6), 389–393 (1982)
9. A.D. Linde, Chaotic inflation. Phys. Lett. B **129**(3–4), 177–181 (1983)
10. F. Lucchin, S. Matarrese, Power-law inflation. Phys. Rev. D **32**(6), 1316 (1985)
11. D. La, P.J. Steinhardt, Extended inflationary cosmology. Phys. Rev. Lett. **62**(4), 376 (1989)
12. I. Moss, V. Sahni, Anisotropy in the chaotic inflationary universe. Phys. Lett. B **178**(2–3), 159–162 (1986)
13. M. Sasaki, Large scale quantum fluctuations in the inflationary universe. Prog. Theor. Phys. **76**(5), 1036–1046 (1986)
14. A.R. Liddle, P. Parsons, J.D. Barrow, Formalizing the slow-roll approximation in inflation. Phys. Rev. D **50**(12), 7222 (1994)
15. W.H. Kinney, Hamilton-Jacobi approach to non-slow-roll inflation. Phys. Rev. D **56**(4), 2002 (1997)
16. S. Nojiri, S.D. Odintsov, V.K. Oikonomou, Constant-roll inflation in F (R) gravity. Class. Quantum Gravity **34**(24), 245012 (2017)
17. A. Awad et al., Constant-roll inflation in f (T) teleparallel gravity. J. Cosmol. Astropart. Phys. **07**(2018), 026 (2018)
18. H. Motohashi, A.A. Starobinsky, f (R) constant-roll inflation. Eur. Phys. J. C **77**, 1–8 (2017)
19. S.D. Odintsov, V.K. Oikonomou, The reconstruction of f (ϕ) R and mimetic gravity from viable slow-roll inflation. Nucl. Phys. B **929**, 79–112 (2018)
20. M. Gamonal, Slow-roll inflation in f (R, T) gravity and a modified Starobinsky-like inflationary model. Phys. Dark Universe **31**, 100768 (2021)
21. S. Bhattacharjee et al., Inflation in f (R, T) gravity. Eur. Phys. J. Plus **135**(7), 576 (2020)

22. H. Motohashi, A.A. Starobinsky, J. Yokoyama, Inflation with a constant rate of roll. J. Cosmol. Astropart. Phys. **2015**(09), 018 (2015)
23. H. Motohashi, A.A. Starobinsky, Constant-roll inflation: confrontation with recent observational data. Europhys. Lett. **117**(3), 39001 (2017)
24. M.J.P. Morse, W.H. Kinney, Large-η constant-roll inflation is never an attractor. Phys. Rev. D **97**(12), 123519 (2018)
25. Z. Yi, Y. Gong, On the constant-roll inflation. J. Cosmol. Astropart. Phys. **2018**(03), 052 (2018)
26. J.T.G. Ghersi, A. Zucca, A.V. Frolov, Observational constraints on constant roll inflation. J. Cosmol. Astropart. Phys. **2019**(05), 030 (2019)
27. Q. Gao, Y. Gong, Z. Yi, On the constant-roll inflation with large and small ηH. Universe **5**(11), 215 (2019)
28. N. Rashidi, M. Heidarzadeh, K. Nozari, Constant-roll inflation with hilltop potential. Eur. Phys. J. Plus **137**(4), 1–9 (2022)
29. H. Rund, *The Differential Geometry of Finsler Spaces*, vol. 101 (Springer Science & Business Media, Berlin, 2012)
30. P.L. Antonelli, R.S. Ingarden, M. Matsumoto, *The Theory of Sprays and Spaces with Applications in Physics and Biology*, vol. 58 (Springer Science & Business Media, Berlin, 1993)
31. B. David, S.-S. Chern, Z. Shen, *An Introduction to Riemann–Finsler Geometry*, vol. 200 (Springer Science & Business Media, Berlin, 2000)
32. K. Lin, S.Z. Yang, A model with exact inflationary solution in Finsler universe. Int. J. Theor. Phys. **48**, 1882–1886 (2009)
33. A.P. Kouretsis, M. Stathakopoulos, P.C. Stavrinos, Covariant kinematics and gravitational bounce in Finsler space-times. Phys. Rev. D **86**(12), 124025 (2012)
34. Z. Chang, S. Wang, Inflation and primordial power spectra at anisotropic spacetime inspired by Planck's constraints on isotropy of CMB. Eur. Phys. J. C **73**, 1–8 (2013)
35. X. Li, S. Wang, Z. Chang, Anisotropic inflation in the Finsler spacetime. Eur. Phys. J. C **75**, 1–8 (2015)
36. X. Li, S. Wang, Primordial power spectrum of tensor perturbations in Finsler spacetime. Eur. Phys. J. C **76**, 1–7 (2016)
37. Z. Nekouee et al., Finsler–Randers model for anisotropic constant-roll inflation. Eur. Phys. J. Plus **137**(12), 1388 (2022)
38. M. Matsumoto, Theory of Finsler spaces with (α, β)-metric. Rep. Math. Phys. **31**(1), 43–83 (1992)
39. V.S. Sabau, H. Shimada, Classes of Finsler spaces with (α, β)-metrics. Rep. Math. Phys. **47**(1), 31–48 (2001)
40. C. Shibata, On Finsler spaces with Kropina metric. Rep. Math. Phys. **13**(1), 117–128 (1978)
41. R.S. Ingarden, M. Matsumoto, ON the 1953 Barthel connection of a Finsler-space and its physical aspect. Publ. Math. Debr. **43**(1–2), 87–90 (1993)
42. R.S. Ingarden, L. Tamássy, The point Finsler spaces and their physical applications in electron optics and thermodynamics. Math. Comput. Model. **20**(4–5), 93–107 (1994)
43. M. Matsumoto, Theory of $ Y $-extremal and minimal hypersurfaces in a Finsler space, On Wegener's and Barthel's theories. J. Math. Kyoto Univ. **26**(4), 647–665 (1986)
44. R.S. Ingarden, M. Matsumoto, On the 1953 Barthel connection of a Finsler space and its mathematical and physical interpretation. Rep. Math. Phys. **32**(1), 35–48 (1993)
45. L. Kozma, On osculation of Finsler-type connections. Acta Math. Hung. **53**(3–4), 389–397 (1989)
46. R. Hama, T. Harko, S.V. Sabau, Dark energy and accelerating cosmological evolution from osculating Barthel–Kropina geometry. Eur. Phys. J. C **82**(4), 385 (2022)
47. A. Bouali et al., Cosmological tests of the osculating Barthel–Kropina dark energy model. Eur. Phys. J. C **83**(2), 121 (2023)
48. Y. Akrami et al., Planck 2018 results-X. Constraints on inflation. Astron. Astrophys. **641**, A10 (2020)
49. S. Castello, S. Ilić, M. Kunz, Updated dark energy view of inflation. Phys. Rev. D **104**(2), 023522 (2021)
50. J.-Q. Xia, X. Zhang, Constraining slow-roll inflation in the presence of dynamical dark energy. Phys. Lett. B **660**(4), 287–292 (2008)
51. S. Ilić et al., Dark energy view of inflation. Phys. Rev. D **81**(10), 103502 (2010)
52. S. Basilakos et al., Resembling dark energy and modified gravity with Finsler–Randers cosmology. Phys. Rev. D **88**(12), 123510 (2013)
53. Z. Chang, X. Li, Modified Friedmann model in Randers–Finsler space of approximate Berwald type as a possible alternative to dark energy hypothesis. Phys. Lett. B **676**(4–5), 173–176 (2009)